PNAS RESEARCH ARTICLE | IMMUNOLOGY AND INFLAMMATION

CD47 promotes peripheral T cell survival by preventing dendritic cell–mediated T cell necroptosis

Satomi Komori[a,b], Yasuyuki Saito[b,1], Taichi Nishimura[b], Datu Respatika[b,c], Hiromi Endoh[d], Hiroki Yoshida[b], Risa Sugihara[b], Rie Iida-Norita[b], Tania Afroj[a,b], Tomoko Takai[a,b], Okechi S. Oduori[a,b], Eriko Nitta[d], Takenori Kotani[b], Yoji Murata[b], Yoriaki Kaneko[e], Ryo Nitta[d], Hiroshi Ohnishi[f], and Takashi Matozaki[a,b,1]

Edited by Jonathan Sprent, Garvan Institute of Medical Research, Darlinghurst, NSW; received March 31, 2023; accepted July 6, 2023

Conventional dendritic cells (cDCs) are required for peripheral T cell homeostasis in lymphoid organs, but the molecular mechanism underlying this requirement has remained unclear. We here show that T cell–specific CD47-deficient ($Cd47^{\Delta T}$) mice have a markedly reduced number of T cells in peripheral tissues. Direct interaction of CD47-deficient T cells with cDCs resulted in activation of the latter cells, which in turn induced necroptosis of the former cells. The deficiency and cell death of T cells in $Cd47^{\Delta T}$ mice required expression of its receptor signal regulatory protein α on cDCs. The development of $CD4^+$ T helper cell–dependent contact hypersensitivity and inhibition of tumor growth by cytotoxic $CD8^+$ T cells were both markedly impaired in $Cd47^{\Delta T}$ mice. CD47 on T cells thus likely prevents their necroptotic cell death initiated by cDCs and thereby promotes T cell survival and function.

T cell | dendritic cell | necroptosis | SIRPα | CD47

Significance

Homeostasis of peripheral T cells is thought to be regulated by conventional dendritic cells (cDCs). However, the molecular mechanisms of such homeostasis have been poorly understood. We here demonstrate that the ablation of CD47 on T cells results in a marked reduction of T cells in the peripheral tissues. CD47-deficient T cells undergo necroptosis through interaction with cDCs. SIRPα on cDCs is required for the induction of T cell necroptosis. Our findings reveal that CD47 on T cells promotes peripheral T cell survival and their function of adaptive immune responses.

Dendritic cells (DCs) are dedicated antigen-presenting cells and orchestrate T cell–mediated immune responses and tolerance (1, 2). They comprise two major subsets, plasmacytoid DCs and conventional DCs (cDCs), with the latter being further divided into type 1 and type 2 cDCs (cDC1s and cDC2s, respectively). In secondary lymphoid organs (SLOs), cDCs promote the proliferation and differentiation of T cells and thereby give rise to effective antigen-specific adaptive immune responses (3). By contrast, cDCs located in the thymus as well as those in peripheral tissues are thought to contribute to the elimination of autoreactive T cells by presenting self-antigens, resulting in the establishment of central or peripheral T cell tolerance (4, 5). Moreover, cDCs play an important role in the survival of peripheral T cells in SLOs by regulating stromal cells such as fibroblastic reticular cells (6, 7). However, the molecular mechanism by which cDCs regulate peripheral T cell survival and homeostasis has not been fully understood.

CD47 is an immunoglobulin superfamily pentatransmembrane protein that is ubiquitously expressed in hematopoietic cells, including red blood cells (RBCs) and lymphocytes (8). The extracellular region of CD47 binds to signal regulatory protein α (SIRPα), which is predominantly expressed on macrophages and cDC2s, resulting in activation of the protein tyrosine phosphatase Shp1, which binds to the cytoplasmic region of SIRPα (9, 10). CD47 on RBCs prevents phagocytosis of these cells and thereby promotes their survival, with this effect of CD47 having been thought to be mediated by its binding to SIPRα on phagocytes (11). The first indication of such a function for CD47 was provided by the observation that the transfer of RBCs from CD47-deficient ($Cd47^{-/-}$) mice to wild-type (WT) mice resulted in the rapid elimination of the $Cd47^{-/-}$ RBCs from the bloodstream of the recipients (12). Depletion of splenic red pulp macrophages (SRPMs) in the recipient mice markedly attenuated this loss of transferred $Cd47^{-/-}$ RBCs. Moreover, the phagocytosis of $Cd47^{-/-}$ RBCs by WT SRPMs in vitro was greatly enhanced compared with that of WT RBCs (13).

Despite these observations suggestive of a key physiological role for CD47-SIRPα signaling, mice lacking CD47 or SIRPα were found to manifest no substantial defects in RBCs or other circulating blood cells in the steady state (12). Indeed, the transfer of $Cd47^{-/-}$ RBCs into $Cd47^{-/-}$ mice failed to result in the rapid elimination of the donor cells (12, 13). In addition, transferred WT or $Cd47^{-/-}$ RBCs were not rapidly eliminated from the bloodstream of SIRPα-deficient recipient mice (14, 15). These findings suggested that CD47 on target blood cells prevents their elimination by phagocytes through an as yet unknown mechanism, such as inhibition of the expression or function of a prophagocytic ligand for phagocytes (15, 16). Indeed, transfer of $Cd47^{-/-}$ RBCs or lymphocytes was shown to result in the activation of DCs, in particular cDC2s, in WT recipients (17, 18). However, it has remained unknown whether such activation of DCs contributes to the rapid elimination of transferred CD47-deficient blood cells from WT recipient mice.

Author contributions: S.K. and Y.S. designed research; S.K., Y.S., T.N., D.R., H.E., H.Y., R.S., R.I.-N., T.A., T.T., O.S.O., and E.N. performed research; S.K., Y.S., T.K., Y.M., Y.K., R.N., and H.O. analyzed data; and S.K., Y.S., and T.M. wrote the paper.

The authors declare no competing interest.

This article is a PNAS Direct Submission.

[1]To whom correspondence may be addressed. Email: ysaito@med.kobe-u.ac.jp or matozaki@med.kobe-u.ac.jp.

This article contains supporting information online at https://www.pnas.org/lookup/suppl/doi:10.1073/pnas.2304943120/-/DCSupplemental.

Published August 7, 2023.

Transfer of *Cd47*$^{-/-}$ lymphocytes also resulted in their rapid elimination from WT recipient mice (19, 20), suggesting that CD47 on lymphocytes is likely important for promotion of their survival in a manner dependent on its interaction with innate cells such as macrophages and DCs. It has remained unknown, however, whether genetic depletion of CD47 in any specific type of lymphocyte, such as T cells, indeed results in their deficiency in mice. Neither effector cells nor molecular mechanisms for such a deficiency have been identified. To address these issues, we have here generated and analyzed T cell–specific CD47 conditional knockout mice. Our findings have revealed a mechanism by which T cells promote their own survival and function by preventing cDC2 activation that results in T cell necroptosis.

Results

Marked Depletion of T Cells in Peripheral Tissues, but Not in the Thymus, of T Cell–Specific CD47-Deficient Mice. We generated mice in which CD47 is specifically ablated in T cells (*Cd47*$^{\Delta T}$ mice) by crossing mice with floxed alleles of *Cd47* (*Cd47*$^{f/f}$ mice) with *Lck*-Cre mice, which express Cre recombinase under the control of the proximal promoter of *Lck*. The expression of *Lck* becomes up-regulated after double-negative stage 3 (DN3 stage) of thymocytes during T cell development in the thymus of adult mice (21). We confirmed that the expression of CD47 in thymocytes was markedly decreased at the DN4 stage, but not at DN1–DN3 stages, in the thymus of *Cd47*$^{\Delta T}$ mice, compared with that apparent for control *Cd47*$^{f/f}$ mice, and that it was minimal at the double-positive (DP) and single-positive (SP) stages (Fig. 1*A*). In addition, the expression of CD47 was minimal in CD4$^+$ and CD8$^+$ T cells of the spleen as well as of peripheral lymph nodes (pLNs) in *Cd47*$^{\Delta T}$ mice (Fig. 1*A*). In contrast, the expression level of CD47 in other immune cell types in the spleen of *Cd47*$^{\Delta T}$ mice was similar to that for control *Cd47*$^{f/f}$ mice (*SI Appendix*, Fig. S1*A*), suggesting that CD47 was specifically ablated in certain thymocytes as well as in peripheral T cells of *Cd47*$^{\Delta T}$ mice.

We next examined the populations of thymocytes and peripheral T cells in *Cd47*$^{\Delta T}$ mice. No gross alteration of thymocyte development was apparent, as revealed by the proportions and absolute numbers of DN, DP, as well as CD4$^+$ and CD8$^+$ SP thymocytes in *Cd47*$^{\Delta T}$ mice compared with those in control *Cd47*$^{f/f}$ mice (Fig. 1*B*). In contrast, the absolute number of total CD3ε$^+$ T cells

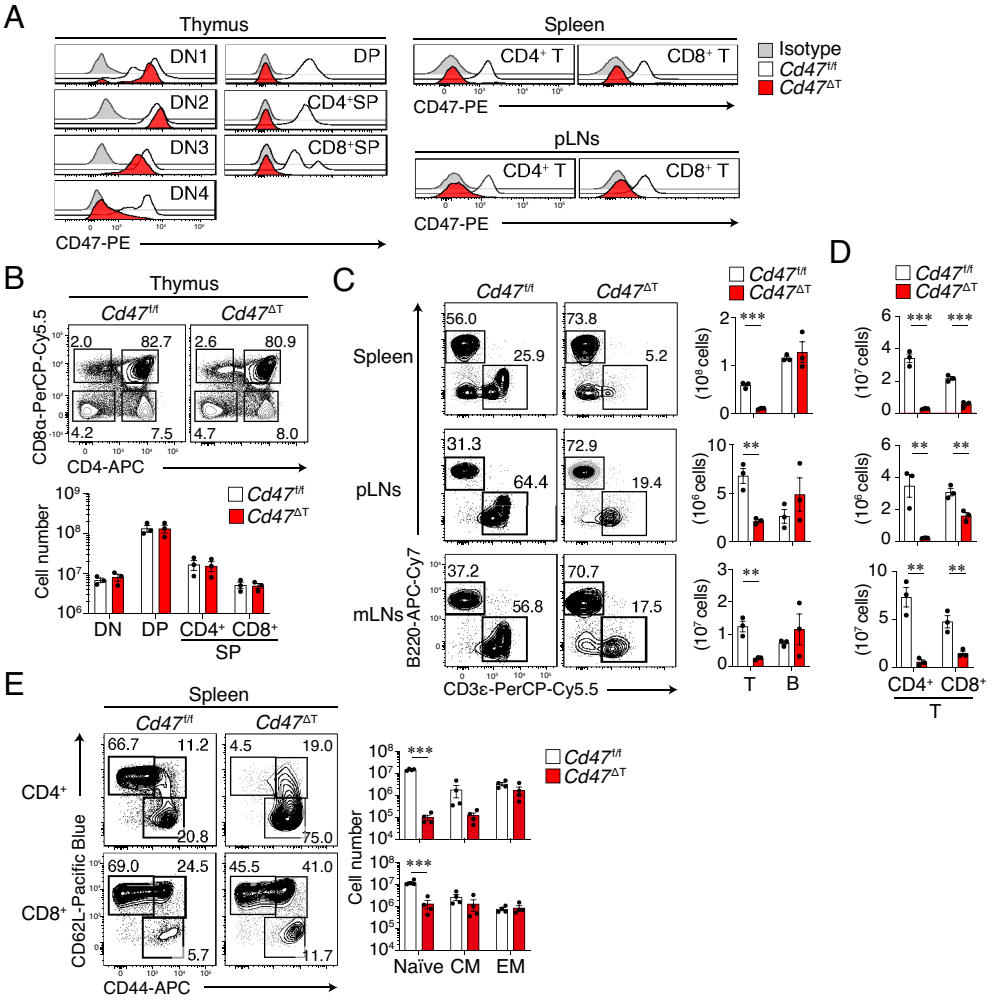

Fig. 1. Marked reduction of T cells in peripheral tissues, but not in the thymus, of T cell–specific CD47-deficient mice. (*A*) Representative histograms for CD47 expression among thymocyte and T cell subsets in *Cd47*$^{f/f}$ or *Cd47*$^{\Delta T}$ mice. (*B*) Representative plots for DN (CD4$^-$CD8$^-$), DP (CD4$^+$CD8$^+$), CD4$^+$ SP, and CD8$^+$ SP thymocytes (*Upper*) and the absolute number of these cells (*Lower*) in *Cd47*$^{f/f}$ or *Cd47*$^{\Delta T}$ mice. (*C*) Representative plots (*Left*) and the absolute number (*Right*) of CD3ε$^+$ T cells and B220$^+$ B cells in the spleen, pLNs, and mLNs of *Cd47*$^{f/f}$ or *Cd47*$^{\Delta T}$ mice. (*D*) Absolute number of CD4$^+$ and CD8$^+$ subsets among CD3ε$^+$ T cells in the spleen, pLNs, and mLNs of *Cd47*$^{f/f}$ or *Cd47*$^{\Delta T}$ mice. (*E*) Representative plots (*Left*) and absolute number (*Right*) of naïve (CD62L$^+$CD44$^-$), central memory (CM, CD62L$^+$CD44$^+$), and effector memory (EM, CD62L$^-$CD44$^+$) T cell subsets in the spleen of *Cd47*$^{f/f}$ or *Cd47*$^{\Delta T}$ mice. Data in *A* are representative of three independent experiments, and cell numbers in *B–E* are pooled from three independent experiments and expressed as mean ± SE values for three or four mice per group. $^{**}P < 0.01$, $^{***}P < 0.001$ (Student's *t* test) in *C–E*.

(Fig. 1*C*) as well as that of $CD4^+$ and $CD8^+$ T cells (Fig. 1*D*) in the spleen, pLNs, and mesenteric LNs (mLNs) was markedly reduced in $Cd47^{\Delta T}$ mice compared with $Cd47^{f/f}$ mice, whereas the absolute number of $B220^+$ B cells was similar between mice of the two genotypes (Fig. 1*C*). In addition, a reduction in the number of total $CD3\varepsilon^+$ T cells as well as that of $CD4^+$ and $CD8^+$ T cells was observed in peripheral blood of $Cd47^{\Delta T}$ mice (*SI Appendix*, Fig. S1*B*). Specific depletion of T cells was also evident in peripheral organs such as the lung and liver of $Cd47^{\Delta T}$ mice (*SI Appendix*, Fig. S1*C*). The absolute number of $Foxp3^+CD25^+$ regulatory T cells was reduced in the spleen of $Cd47^{\Delta T}$ mice compared with that apparent for $Cd47^{f/f}$ mice (*SI Appendix*, Fig. S1*D*), although the frequency of the subset among $CD4^+$ T cells was relatively increased in $Cd47^{\Delta T}$ mice. Together, these results suggested that CD47 is essential for the homeostatic regulation of mature T cells in peripheral tissues. To clarify whether the selective reduction of T cells depends on the deficiency of CD47 on T cells, we next generated mixed bone marrow (BM) chimeras by transferring mixed (1:1 ratio) BM from WT or $Cd47^{\Delta T}$ ($CD45.2^+$) and WT ($CD45.1^+$) mice into lethally irradiated WT ($CD45.1^+/45.2^+$) recipients (*SI Appendix*, Fig. S1*E*). Compared with T cells derived from WT:WT mixed donor BM cells, $Cd47^{\Delta T}$:WT mixed BM chimeras manifested selective reduction of $CD45.2^+$ T cells in the spleen (*SI Appendix*, Fig. S1*E*). Moreover, the reduction of peripheral T cells was not observed in *Lck*-Cre;$Cd47^{f/+}$ mice (*SI Appendix*, Fig. S1*F*). Thus, the ablation of CD47 in T cells caused selective loss of CD47–deficient T cells in peripheral tissues.

We also examined the frequency of T cell subpopulations such as naïve, central memory, and effector memory T cells in SLOs of $Cd47^{\Delta T}$ mice. Both the frequency and absolute number of naïve $CD4^+$ or $CD8^+$ T cells were greatly reduced in both the spleen (Fig. 1*E*) and pLNs (*SI Appendix*, Fig. S1*G*) of $Cd47^{\Delta T}$ mice compared with those apparent for $Cd47^{f/f}$ mice. By contrast, the absolute number of effector memory or central memory $CD4^+$ or $CD8^+$ T cells in the spleen (Fig. 1*E*) or pLNs (*SI Appendix*, Fig. S1*G*) did not differ between $Cd47^{\Delta T}$ and $Cd47^{f/f}$ mice.

Increased Turnover and Activation of, as well as Gene Expression Related to Inflammation and Cell Death in, T Cells of $Cd47^{\Delta T}$ Mice. We next examined the turnover of T cells in the spleen of $Cd47^{\Delta T}$ mice by monitoring the kinetics of cell labeling with bromodeoxyuridine (BrdU) in the continuous presence of this agent (22). Whereas 19.2 ± 0.7% and 21.4 ± 0.7% (mean ± SE) of $CD4^+$ or $CD8^+$ T cells, respectively, in the spleen of $Cd47^{f/f}$ mice were labeled with BrdU at 14 d after the onset of exposure to this agent, 62.8 ± 5.1% and 50.7 ± 5.9% of the corresponding cells in the spleen of $Cd47^{\Delta T}$ mice were so labeled (Fig. 2*A*). BrdU labeling of $CD4^+$ or $CD8^+$ T cells in pLNs of $Cd47^{\Delta T}$ mice was also greater than that apparent for $Cd47^{f/f}$ mice (*SI Appendix*, Fig. S2*A*), suggesting that the turnover of $CD4^+$ and $CD8^+$ T cells was markedly increased in SLOs of $Cd47^{\Delta T}$ mice. Consistent with these findings, analysis of cell cycle status of T cells revealed that the proportion of splenic $CD4^+$ or $CD8^+$ T cells in G_0 phase (quiescent cells) was greatly reduced, whereas that of those in interphase (G_1 or S-G_2-M phases) was increased, in the spleen of $Cd47^{\Delta T}$ mice compared with that of $Cd47^{f/f}$ mice (*SI Appendix*, Fig. S2*B*). Furthermore, the expression of CD69 or programmed cell death–1 (PD-1), both of which reflect the activation state of T cells, was significantly elevated in the remaining splenic T cells, in particular in the $CD4^+$ subset, of $Cd47^{\Delta T}$ mice (Fig. 2*B*).

To characterize further the changes to peripheral T cells in $Cd47^{\Delta T}$ mice, we performed RNA-sequencing (RNA-seq) analysis of sorted T cells from the spleen of these mice as well as that of $Cd47^{f/f}$ mice. $Cd47^{\Delta T}$ T cells manifested 1,257 differentially expressed genes (DEGs, 1,159 up-regulated and 98 down-regulated) relative to $Cd47^{f/f}$ T cells. A volcano plot showed that the expression of *Cd38*, *Pdcd1* (encoding PD-1), *Il10*, *Havcr2* (encoding Tim3), and *Lag3* was markedly increased in $Cd47^{\Delta T}$ T cells compared with $Cd47^{f/f}$ T cells (Fig. 2*C*). Gene set enrichment analysis (GSEA) showed that $Cd47^{\Delta T}$ T cells were more enriched in genes for the inflammatory response compared with $Cd47^{f/f}$ T cells (Fig. 2*D*). In addition, $Cd47^{\Delta T}$ T cells were more enriched in genes for positive regulation of cell death compared with $Cd47^{f/f}$ T cells (Fig. 2*D*). Indeed, heat map analysis showed that DEGs specifically up-regulated in $Cd47^{\Delta T}$ T cells included many genes associated with inflammation (*Il10*, *Cxcl10*, *Nlrp3*, *Tnfrsf9*, *Tnfrsf1b*) or cell death (*Casp3*, *Anxa1*, *Dapk2*, *Adam8*, *Bard1*, *Pmaip1*) compared with $Cd47^{f/f}$ T cells (Fig. 2*E*). These results thus suggested that T cells remaining in the spleen of $Cd47^{\Delta T}$ mice manifested activated and inflammatory states that were likely related to cell death.

Necroptotic Cell Death of Peripheral T Cells in $Cd47^{\Delta T}$ Mice. Given that expression of genes related to cell death was prominent in peripheral T cells of $Cd47^{\Delta T}$ mice, we next investigated whether cell death indeed occurs—and, if so, what type—in these cells. Indeed, the frequency of Annexin V^+ T cells in both the spleen (Fig. 3*A*) and pLNs (*SI Appendix*, Fig. S3*A*) was greatly increased in $Cd47^{\Delta T}$ mice compared with $Cd47^{f/f}$ mice. In addition, the mitochondrial membrane potential ($\Delta\psi_m$), which was measured on the basis of aggregation of the mitochondrial membrane dye JC-1, was markedly reduced in $CD4^+$ T cells in the spleen of $Cd47^{\Delta T}$ mice compared with that of $Cd47^{f/f}$ mice (*SI Appendix*, Fig. S3*B*). Moreover, the abundance of reactive oxygen species (ROS) (Fig. 3*B*) as well as the expression of Fas (Fig. 3*C*) was significantly increased in splenic T cells from $Cd47^{\Delta T}$ mice compared with those from $Cd47^{f/f}$ mice, suggesting that regulated cell death occurs in splenic T cells of $Cd47^{\Delta T}$ mice (23).

Several types of regulated cell death, including apoptosis, necroptosis, and pyroptosis, have been described (24). Apoptosis is a caspase-dependent form of cell death, characterized by cytoplasmic shrinkage, chromatin condensation, and nuclear fragmentation. By contrast, necroptosis is a caspase-independent type of cell death, characterized by increased cell volume, translucent cytoplasm with focal ruptures of the plasma membrane, organelle swelling, and intact nuclei (25, 26). Light microscopic examination with May-Grünwald–Giemsa staining of sorted splenic T cells showed that most of the remaining T cells of $Cd47^{\Delta T}$ mice appeared fragile and that the ratio of bursted cells was markedly increased compared with that for $Cd47^{f/f}$ mice (Fig. 3*D*). Transmission electron microscopy (TEM) also revealed that the remaining T cells in the spleen and pLNs of $Cd47^{\Delta T}$ mice typically manifested an increased size as well as swelling of cytoplasmic organelles and decreased condensation of chromatin compared with T cells of $Cd47^{f/f}$ mice (Fig. 3*E*). These results suggested that the cell death apparent for T cells in $Cd47^{\Delta T}$ mice morphologically resembled necroptosis. In contrast, the expression of apoptosis-related genes such as *Casp8*, *Bax*, and *Bcl2* was not increased in splenic T cells from $Cd47^{\Delta T}$ mice compared with those from $Cd47^{f/f}$ mice (*SI Appendix*, Fig. S3*C*). Moreover, the main effectors of apoptotic cell death, including caspase-8 and caspase-3, remained in the inactive proenzyme form in T cells of $Cd47^{\Delta T}$ mice (*SI Appendix*, Fig. S3*D*), suggesting that the increased cell death of these cells is not likely attributable to caspase-dependent apoptosis.

The phosphorylation and oligomerization of mixed-lineage kinase domain–like (MLKL), a pseudokinase downstream of phosphorylated receptor-interacting protein kinase 3 (RIP3), are

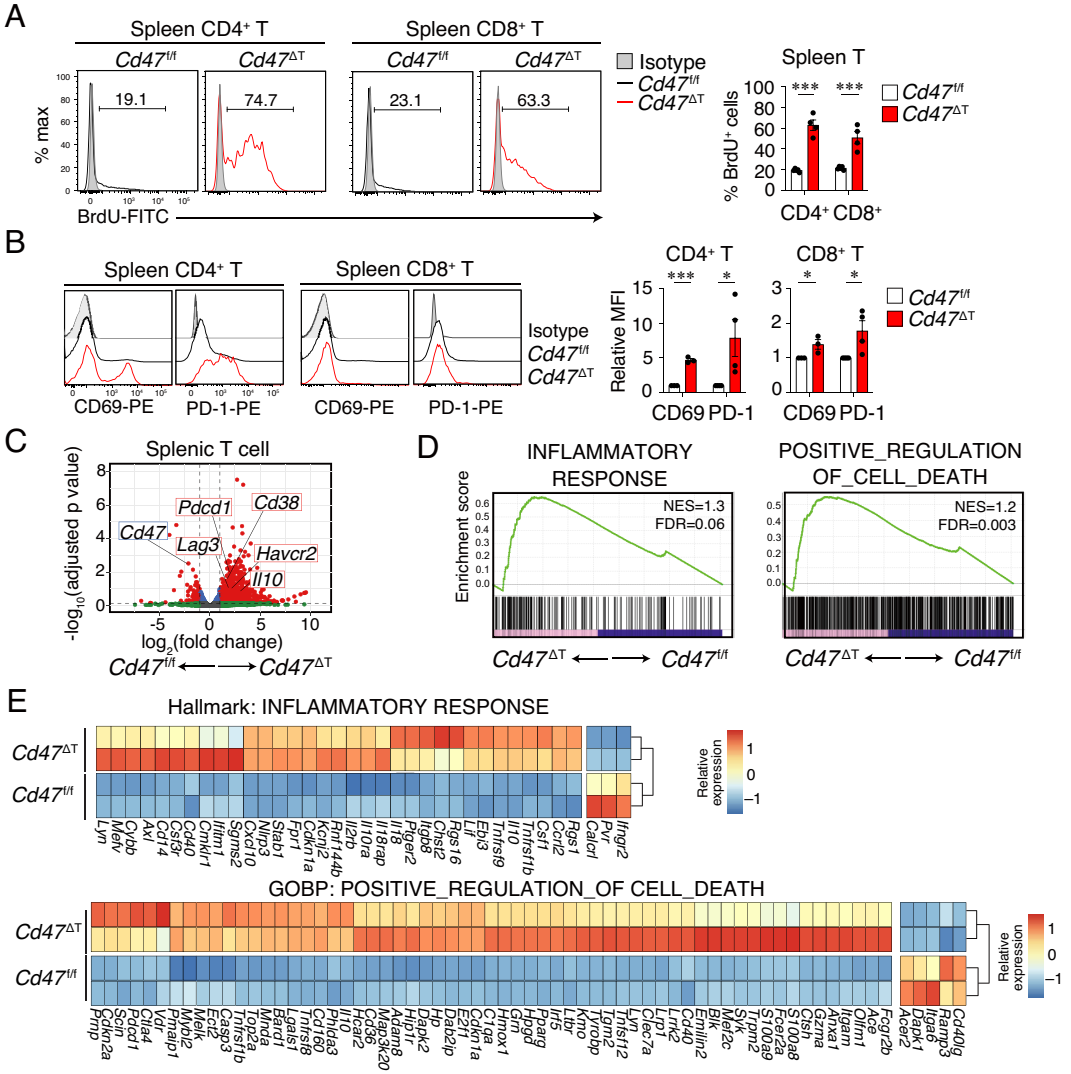

Fig. 2. Increased turnover and activation of, as well as gene expression related to inflammation and cell death in, T cells of *Cd47*$^{\Delta T}$ mice. (*A*) Representative histograms (*Left*) and proportions (*Right*) of BrdU$^+$ cells among CD4$^+$ or CD8$^+$ T cells in the spleen of *Cd47*$^{f/f}$ or *Cd47*$^{\Delta T}$ mice treated with BrdU for 14 d. (*B*) Representative histograms (*Left*) and the relative mean fluorescence intensity (MFI, *Right*) for CD69 or PD-1 expression among CD4$^+$ or CD8$^+$ T cells in the spleen of *Cd47*$^{f/f}$ or *Cd47*$^{\Delta T}$ mice. Data in the *Right* panels of *A* and *B* are mean ± SE values for three-to-five mice per group and are pooled from three independent experiments. *$P < 0.05$, ***$P < 0.001$ (Student's *t* test). (*C–E*) RNA-seq analysis was performed for sorted splenic T cells from *Cd47*$^{f/f}$ or *Cd47*$^{\Delta T}$ mice (n = 2). (*C*) Volcano plot showing differential gene expression in *Cd47*$^{\Delta T}$ T cells relative to *Cd47*$^{f/f}$ T cells. (*D*) GSEA of pairwise comparisons of T cells between *Cd47*$^{\Delta T}$ and *Cd47*$^{f/f}$ mice. (*E*) Heat maps showing the expression in T cells from *Cd47*$^{\Delta T}$ and *Cd47*$^{f/f}$ mice of DEGs included in the GSEA gene sets in *D*.

thought to be important for the promotion of necroptosis (27). Indeed, the abundance of *Mlkl* mRNA was significantly up-regulated in splenic T cells from *Cd47*$^{\Delta T}$ mice compared with those from *Cd47*$^{f/f}$ mice (Fig. 3*F*). In addition, the abundance of phosphorylated MLKL was markedly increased in both CD4$^+$ and CD8$^+$ splenic T cells from *Cd47*$^{\Delta T}$ mice (Fig. 3*G*). Moreover, the amount of phosphorylated RIP3 was significantly increased in both CD4$^+$ and CD8$^+$ T cells from *Cd47*$^{\Delta T}$ mice compared with those from *Cd47*$^{f/f}$ mice (*SI Appendix*, Fig. S3*E*). To further examine whether the reduction in a number of peripheral T cells was attributable to T cell necroptosis in *Cd47*$^{\Delta T}$ mice, we treated mice with Necrostatin-1 (Nec-1), an allosteric inhibitor specific for RIPK1 in vivo. In contrast to the minimal effect of Nec-1 on *Cd47*$^{f/f}$ T cells, the absolute number of T cells was significantly increased 6 d after the treatment with Nec-1 in the spleen of *Cd47*$^{\Delta T}$ mice (Fig. 3*H* and *SI Appendix*, Fig. S3*F*). Collectively, these results suggested that ablation of CD47 specifically in T cells induces their necroptosis, resulting in a marked deficiency of T cells in *Cd47*$^{\Delta T}$ mice.

Role of cDCs in the Deficiency of T Cells in *Cd47*$^{\Delta T}$ Mice. Transfusion of *Cd47*$^{-/-}$ RBCs into WT mice resulted in their rapid phagocytosis by SRPMs and their elimination from the bloodstream (12, 19). We therefore next examined whether macrophages contribute to the deficiency of peripheral T cells in *Cd47*$^{\Delta T}$ mice. However, depletion of F4/80$^+$CD11b$^+$ SRPMs by clodronate liposome treatment (*SI Appendix*, Fig. S4*A*) failed to increase the reduced number of peripheral T cells in *Cd47*$^{\Delta T}$ mice (*SI Appendix*, Fig. S4*B*). In addition, depletion of granulocytes or natural killer (NK) cells by injection of antibodies to Ly6G or to asialoganglioside GM1, respectively, had no effect on the deficiency of T cells in *Cd47*$^{\Delta T}$ mice (*SI Appendix*, Fig. S4 *C* and *D*).

Given that, after naïve T cells exit the thymus, they first encounter cDCs in SLOs (28), we next examined the effect of CD11c$^+$ DC depletion on the deficiency of T cells in *Cd47*$^{\Delta T}$ mice. To this end, we generated *Cd47*$^{\Delta T}$ mice in which DC depletion is inducible by diphtheria toxin (DTx) administration by crossing *Cd47*$^{\Delta T}$ mice and CD11c$^{iDTR\Delta}$ mice (29). The resulting mice were used

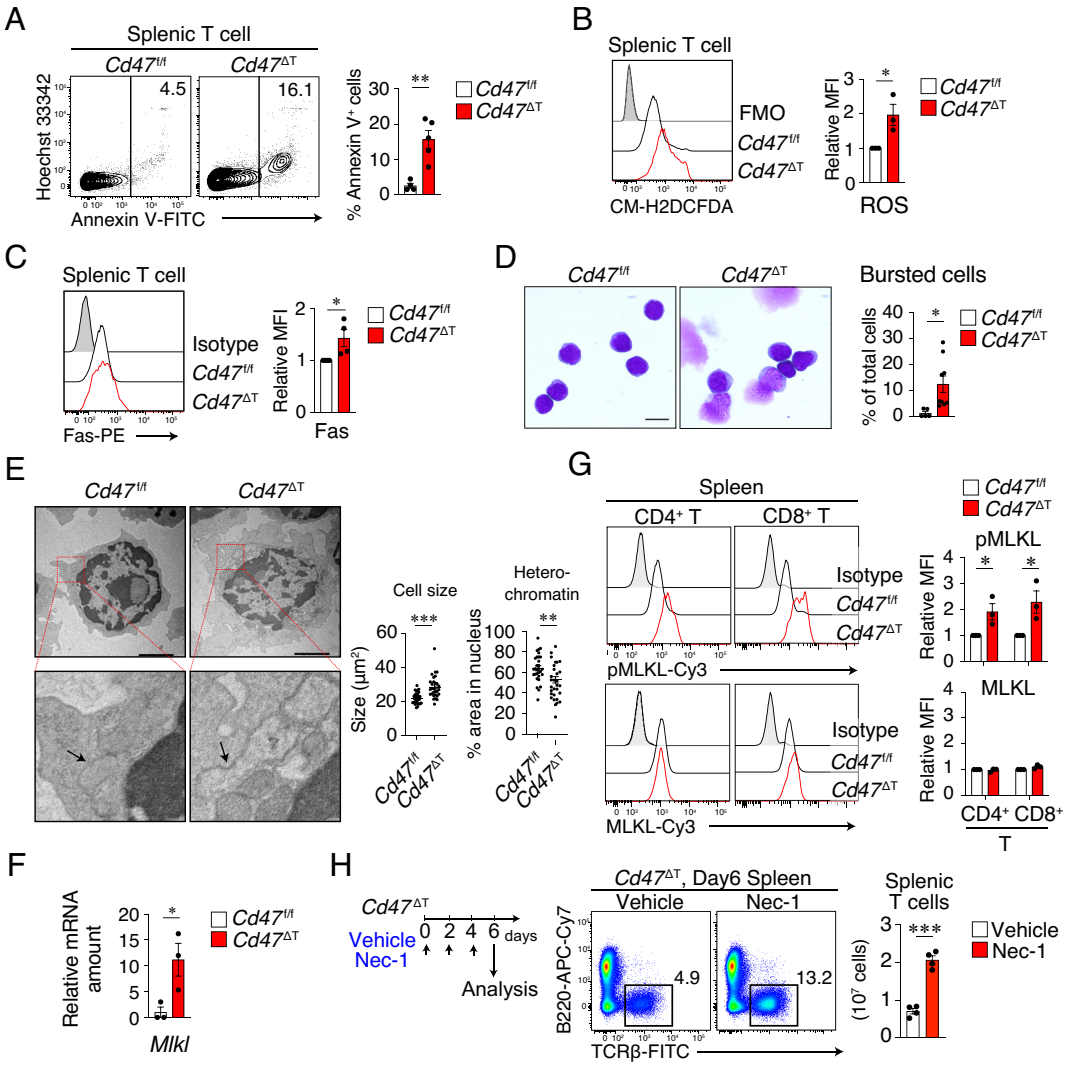

Fig. 3. Necroptotic cell death of peripheral T cells in *Cd47*$^{\Delta T}$ mice. (*A*) Representative flow cytometric profiles (*Left*) and the percentage (*Right*) of Annexin V$^+$ cells among T cells in the spleen of *Cd47*$^{f/f}$ or *Cd47*$^{\Delta T}$ mice. (*B*) Representative plot (*Left*) and the relative MFI of CM-H2DCFDA fluorescence (*Right*) in splenic T cells from *Cd47*$^{f/f}$ or *Cd47*$^{\Delta T}$ mice. Intracellular ROS levels were determined on the basis of CM-H2DCFDA fluorescence. FMO, fluorescence minus one. (*C*) Representative histograms (*Left*) and the relative MFI (*Right*) for Fas expression in splenic T cells from *Cd47*$^{f/f}$ or *Cd47*$^{\Delta T}$ mice. (*D*) May–Grünwald–Giemsa staining of sorted T cells from the spleen of *Cd47*$^{f/f}$ or *Cd47*$^{\Delta T}$ mice. The proportion of bursted cells in each image was counted for each sample. (Scale bar, 5 μm.) (*E*) TEM of sorted T cells from the spleen and pLNs of *Cd47*$^{f/f}$ or *Cd47*$^{\Delta T}$ mice. The boxed areas of the *Upper* images are shown at higher magnification in the *Lower* images. Arrows indicate the cytoplasmic organelles. (Scale bars, 2 μm.) Quantification of cell size as well as the percentage area of heterochromatin in the nucleus is also shown. (*F*) qPCR analysis of *Mlkl* mRNA abundance in splenic T cells from *Cd47*$^{f/f}$ or *Cd47*$^{\Delta T}$ mice. (*G*) Representative profiles (*Left*) and relative MFI (*Right*) for phosphorylated (p) and total forms of MLKL in splenic CD4$^+$ or CD8$^+$ T cells from *Cd47*$^{f/f}$ or *Cd47*$^{\Delta T}$ mice. (*H*) Nec-1 or vehicle was injected into *Cd47*$^{\Delta T}$ mice every other day and the cell number of splenic T cell was analyzed 6 d after the first Nec-1 injection. Data are mean ± SE values for three-to-five mice per group from two-to-four independent experiments (*A–C* and *F–H*), for five-to-nine images obtained from two independent experiments (*D*), or for 30 cells per group (*E*). *P < 0.05, **P < 0.01, ***P < 0.001 (Student's t test).

for the generation of *Cd47*$^{\Delta T}$;CD11c$^{iDTR\Delta}$ BM chimera (hereafter referred to as *Cd47*$^{\Delta T}$;CD11c$^{iDTR\Delta}$). We treated these animals with DTx by intravenous injection on days 0 and 3 (Fig. 4*A*). Such DTx treatment indeed resulted in marked depletion of CD11c$^+$MHCII$^+$(major histocompatibility complex class II$^+$) cDCs, but not of CD11b$^+$F4/80$^+$ macrophages, in the spleen of *Cd47*$^{\Delta T}$;CD11c$^{iDTR\Delta}$ mice (*SI Appendix*, Fig. S4*E*). The percentage of Annexin V$^+$ cells among splenic T cells was significantly smaller for DTx-treated *Cd47*$^{\Delta T}$;CD11c$^{iDTR\Delta}$ mice than for untreated *Cd47*$^{\Delta T}$;CD11c$^{iDTR\Delta}$ mice (Fig. 4*B*). Furthermore, the abundance of phosphorylated MLKL was markedly reduced in T cells from DTx-treated *Cd47*$^{\Delta T}$;CD11c$^{iDTR\Delta}$ mice (Fig. 4*C*), suggesting that necroptosis of peripheral T cells was attenuated by the depletion of cDCs in *Cd47*$^{\Delta T}$;CD11c$^{iDTR\Delta}$ mice. Consistent with these findings, the number of T cells was significantly increased in both the spleen (Fig. 4*D*) and pLNs (*SI Appendix*, Fig. S4*F*) of DTx-treated *Cd47*$^{\Delta T}$;CD11c$^{iDTR\Delta}$ mice compared with those of untreated *Cd47*$^{\Delta T}$;CD11c$^{iDTR\Delta}$ mice or DTx-treated CD11c$^{iDTR\Delta}$ mice (*SI Appendix*, Fig. S4*G*). Given that splenic CD11c$^+$ DCs were not completely depleted 7 d after DTx injection in *Cd47*$^{\Delta T}$;CD11c$^{iDTR\Delta}$ mice (*SI Appendix*, Fig. S4*E*), however, remained DCs likely induced T cell death, which resulted in the partial recovery of T cells after DTx treatment in *Cd47*$^{\Delta T}$;CD11c$^{iDTR\Delta}$ mice. Together, these results thus suggested that cDCs contribute, at least in part, to the induction of necroptotic cell death in CD47-deficient T cells of *Cd47*$^{\Delta T}$ mice.

We next examined and characterized cDCs in *Cd47*$^{\Delta T}$ mice. The frequency as well as the absolute number of CD4$^+$ cDC2s was significantly reduced in the spleen of *Cd47*$^{\Delta T}$ mice compared with that of *Cd47*$^{f/f}$ mice, whereas the frequency and absolute number of CD8α$^+$ cDC1s did not differ between the two genotypes (Fig. 4*E*). By contrast, the expression of CD86 and MHCII

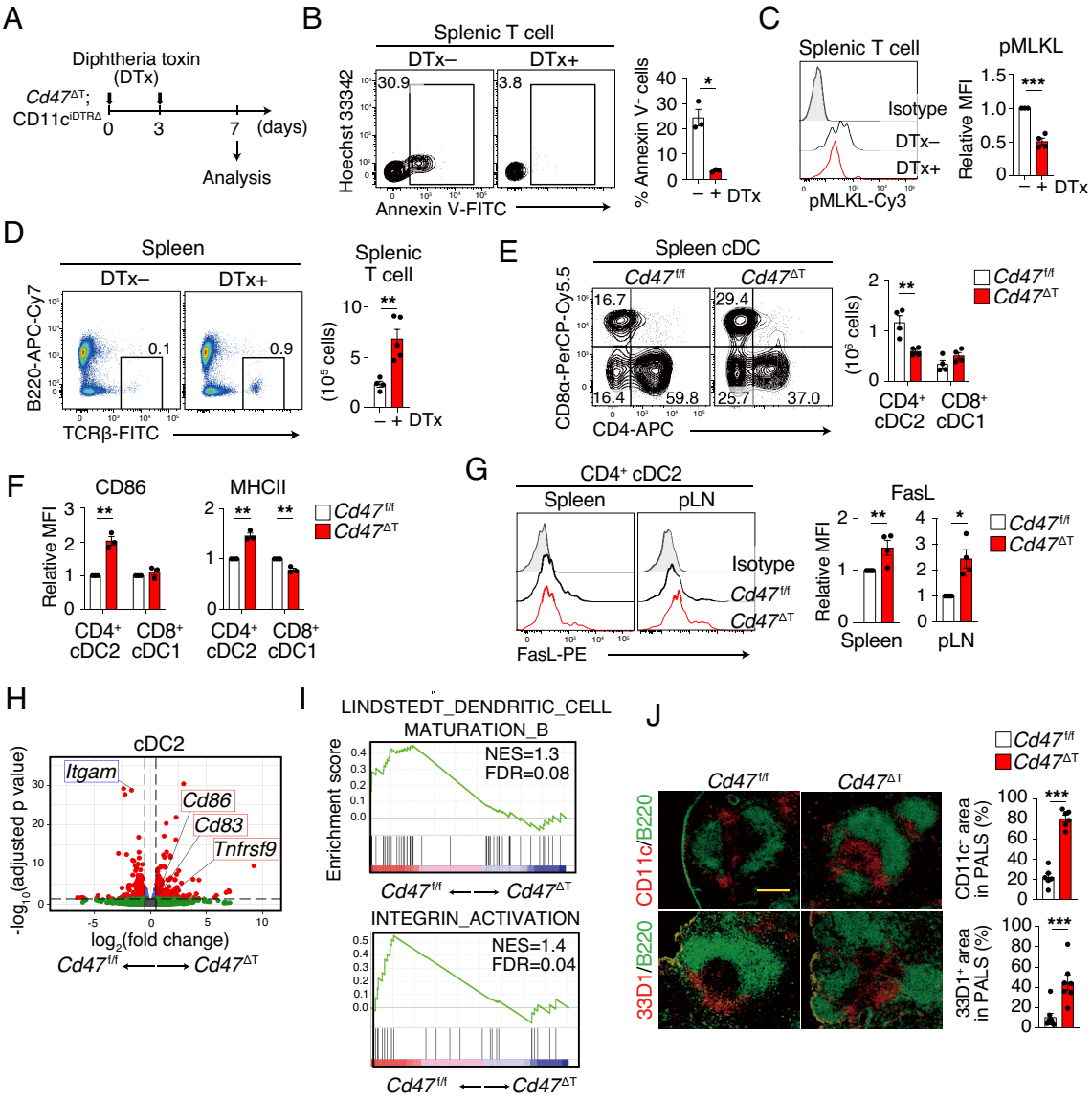

Fig. 4. Role of cDCs in the deficiency of T cells in *Cd47*$^{\Delta T}$ mice. (*A*) Experimental schedule for DTx injection in *Cd47*$^{\Delta T}$;CD11c$^{iDTR\Delta}$ mice. (*B*) Representative flow cytometry plots (*Left*) and frequency (*Right*) of Annexin V$^+$ T cells in the spleen of *Cd47*$^{\Delta T}$;CD11c$^{iDTR\Delta}$ mice without or 7 d after DTx injection. (*C*) Representative flow cytometric profiles (*Left*) and relative MFI (*Right*) for phosphorylated MLKL in splenic T cells from *Cd47*$^{\Delta T}$;CD11c$^{iDTR\Delta}$ mice without or 7 d after DTx injection. (*D*) Representative plots (*Left*) and absolute number (*Right*) of TCRβ$^+$ T cells in the spleen of *Cd47*$^{\Delta T}$;CD11c$^{iDTR\Delta}$ mice without or 7 d after DTx injection. (*E*) Representative plots (*Left*) and absolute number (*Right*) of CD4$^+$ cDC2s or CD8$^+$ cDC1s in the spleen of *Cd47*$^{\Delta T}$ or *Cd47*$^{f/f}$ mice. (*F*) Relative MFI of CD86 and MHCII for CD4$^+$ cDC2s or CD8$^+$ cDC1s isolated from the spleen of *Cd47*$^{f/f}$ or *Cd47*$^{\Delta T}$ mice. (*G*) Relative MFI for expression of FasL in CD4$^+$ cDC2s from the spleen or pLNs of *Cd47*$^{f/f}$ or *Cd47*$^{\Delta T}$ mice. (*H* and *I*) RNA-seq analysis of the cDC2 subset sorted from the spleen of *Cd47*$^{f/f}$ or *Cd47*$^{\Delta T}$ mice. (*H*) Volcano plot of gene expression changes in cDC2s of *Cd47*$^{\Delta T}$ mice relative to *Cd47*$^{f/f}$ mice. (*I*) GSEA for comparison of cDC2s between *Cd47*$^{\Delta T}$ and *Cd47*$^{f/f}$ mice. (*J*) Frozen sections of the spleen from *Cd47*$^{f/f}$ or *Cd47*$^{\Delta T}$ mice were subjected to immunohistofluorescence analysis with antibodies to CD11c or to 33D1 (red) and with those to B220 (green). The percentage CD11c$^+$ or 33D1$^+$ area among PALS in each image was also measured. (Scale bar, 200 μm.) Data are mean ± SE values for three or four mice per group from two independent experiments (*B* and *C*), or for three-to-five mice per group pooled from three or four independent experiments (*D*–*G*, and *J*). *P < 0.05, **P < 0.01, ***P < 0.001 (Student's t test).

was markedly increased in CD4$^+$ cDC2s, but not in cDC1s, from *Cd47*$^{\Delta T}$ mice compared with those from *Cd47*$^{f/f}$ mice (Fig. 4*F*). Such CD86 expression on splenic cDC2s were also up-regulated in *Cd47*$^{\Delta T}$ mice after the treatment of Nec-1 (*SI Appendix*, Fig. S4*H*). In addition, cDC2s showed upregulation of the expression of Fas ligand (FasL) in SLOs of *Cd47*$^{\Delta T}$ mice (Fig. 4*G*). RNA-seq analysis of cDC2s isolated from the spleen of *Cd47*$^{\Delta T}$ mice revealed 468 DEGs (230 up-regulated and 238 down-regulated) relative to those of *Cd47*$^{f/f}$ mice. In addition, the expression of *Tnfrsf9*, *Cd86*, and *Cd83*, all of which are thought to be associated with DC activation (30), was significantly increased, whereas that of *Itgam* (encoding CD11b) was decreased, in cDC2s from *Cd47*$^{\Delta T}$ mice compared with those from *Cd47*$^{f/f}$ mice (Fig. 4*H*). GSEA also showed that cDC2s of *Cd47*$^{\Delta T}$ mice were more enriched in genes associated with DC maturation or integrin activation than were those of *Cd47*$^{f/f}$ mice (Fig. 4*I*). Splenic cDC2s are thought to be present at the marginal zone, in a region known as the bridging channel, in the steady state, whereas they migrate to the T cell zone and interact with T cells after their activation (31). Indeed, immunohistofluorescence analysis showed that cDC2s, detected by staining with antibodies to CD11c or to 33D1, accumulated in the T cell areas (periarteriolar lymphoid sheaths, or PALS) of the spleen in *Cd47*$^{\Delta T}$ mice, whereas most of these cells localized to the marginal zone, in particular at the bridging channel, in the spleen of *Cd47*$^{f/f}$ mice (Fig. 4*J*). These results thus suggested that cDC2s were selectively activated and

markedly reduced in number, presumably as a result of their interaction with CD47-deficient T cells, in SLOs of *Cd47*$^{\Delta T}$ mice. Given that cDCs are required for the loss of T cells in *Cd47*$^{\Delta T}$ mice, activation of cDC2s by CD47-deficient T cells likely in turn promotes the necroptotic cell death of these T cells.

Transfer of *Cd47* $^{-/-}$ T Cells into WT Recipient Mice Results in Their Cell Death and Rapid Elimination as well as in cDC2 Activation. Transfer of lymphoid cells such as T cells from *Cd47*$^{-/-}$ mice into WT mice was previously shown to result in their rapid elimination (20). Indeed, we found that transfer of carboxyfluorescein succinimidyl ester (CFSE)–labeled T cells from *Cd47*$^{-/-}$ mice (they are mostly naïve and viable) (*SI Appendix*, Fig. S5 *A* and *B*) into WT mice resulted in a rapid and marked reduction in the number of CFSE^{+} cells in peripheral blood of the recipients compared with the fate of T cells transferred from WT mice (Fig. 5*A*). Moreover, incorporation of CFSE^{+} *Cd47*$^{-/-}$ T cells into the spleen of WT mice was minimal at 4 h after cell transfer compared with that apparent for T cells transferred from WT mice (Fig. 5*B*). However, transferred CFSE^{+} *Cd47*$^{-/-}$ T cells were not taken up by F4/80^{+} macrophages in the spleen of WT recipients (*SI Appendix*, Fig. S5*C*), suggesting that the clearance of *Cd47*$^{-/-}$ T cells from the recipient mice was unlikely attributable to their phagocytosis by macrophages. By contrast, the frequency of Annexin V^{+} cells among transferred *Cd47*$^{-/-}$ T cells remaining in the spleen was greatly increased at 1 h after cell transfer compared with that apparent for T cells transferred from WT mice (Fig. 5*C*). Moreover, the percentage of burst cells among transferred *Cd47*$^{-/-}$ T cells was markedly increased compared with that for transferred WT T cells (Fig. 5*D*). In contrast, rapid elimination of transferred *Cd47*$^{-/-}$ T cells from peripheral blood was significantly attenuated in DC-depleted (DTx-treated CD11c$^{iDTR\Delta}$) recipient mice (Fig. 5*A*). In addition, transfer of *Cd47*$^{-/-}$ T cells resulted in the upregulation of CD86 and MHCII in splenic cDC2s of WT recipient mice (Fig. 5*E*). The transient transfer of *Cd47*$^{-/-}$ T cells into WT mice thus likely phenocopies *Cd47*$^{\Delta T}$ mice and results in necroptotic cell death of *Cd47*$^{-/-}$ T cells as well as activation of cDC2s, leading to the rapid elimination of the transferred *Cd47*$^{-/-}$ T cells from the blood and spleen of the recipient mice.

To clarify how DCs promote the activation and subsequent cell death of CD47-deficient T cells, we next investigated the importance of SIRPα in cDCs. With the use of DC-specific SIRPα-deficient mice (*Sirpa*$^{\Delta DC}$: *Itgax*-Cre;*Sirpa*$^{f/f}$) (32), we next examined the importance of SIRPα in cDCs for the elimination of as well as the induction of cell death in CD47-deficient T cells transferred into

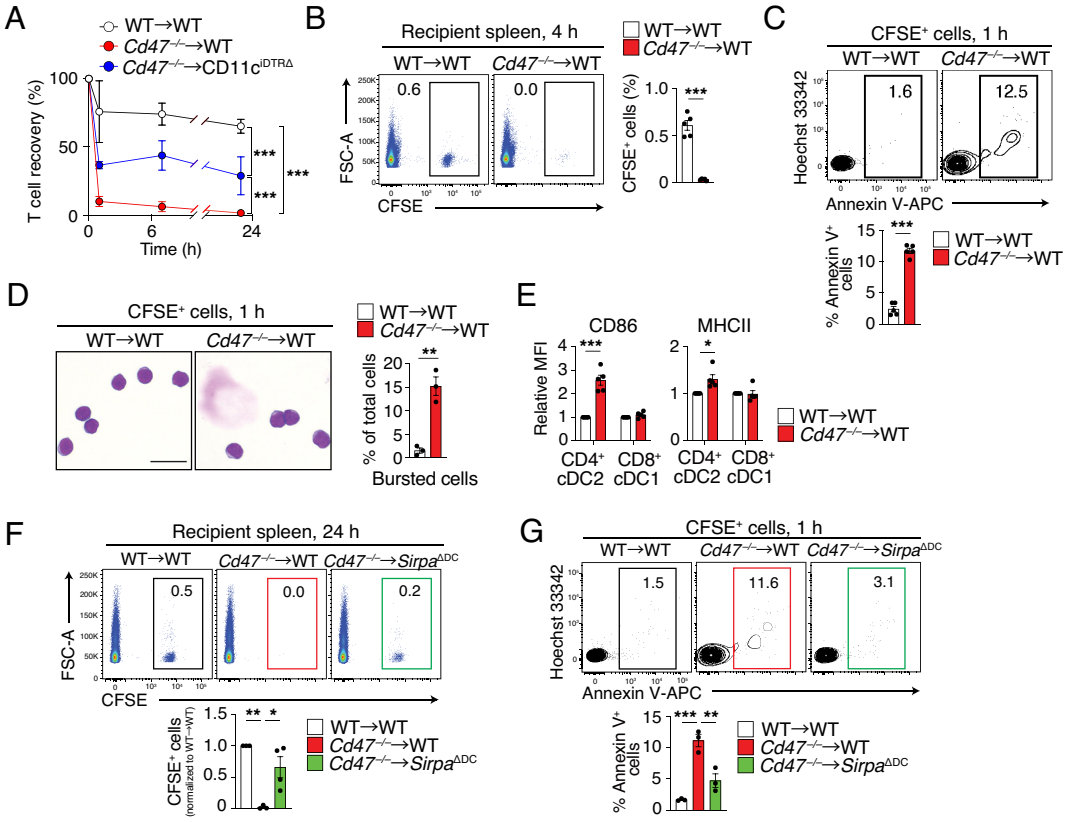

Fig. 5. Transfer of *Cd47* $^{-/-}$ T cells into WT recipient mice results in their cell death and rapid elimination as well as in cDC2 activation. (*A*) T cells isolated from *Cd47* $^{-/-}$ or control WT mice were stained with CFSE and injected into WT or DTx-treated CD11c$^{iDTR\Delta}$ mice, and the frequency of transferred CFSE^{+} T cells among total T cells in peripheral blood of the recipient mice was determined by flow cytometry at the indicated times. Data are normalized to the frequency of CFSE^{+} T cells at 1 h after injection. (*B*) Representative plots (*Left*) and the proportion (*Right*) of CFSE-labeled T cells from *Cd47* $^{-/-}$ or WT mice in the spleen of WT recipient mice at 4 h after cell transfer. (*C*) Representative flow cytometric profiles (*Left*) and the percentage (*Right*) of Annexin V^{+} cells among injected T cells in the spleen of WT recipient mice as in B at 1 h after cell injection. (*D*) May–Grünwald–Giemsa staining of sorted CFSE^{+} cells isolated from the spleen of WT recipient mice at 1 h after cell injection as in *B*. (Scale bar, 5 μm.) The proportion of bursted cells in each image is also shown for each sample. (*E*) Relative MFI of CD86 and MHCII in CD4^{+} cDC2s or CD8^{+} cDC1s in the spleen of WT recipients at 24 h after transfer of WT or *Cd47* $^{-/-}$ T cells. (*F*) Representative plots (*Top*) and frequency (*Bottom*) of CFSE^{+} T cells derived from WT or *Cd47* $^{-/-}$ donor mice among total splenocytes isolated from WT or *Sirpa*$^{\Delta DC}$ recipient mice at 24 h after cell transfer. (*G*) Representative flow cytometric profiles (*Top*) and the percentage (*Bottom*) of Annexin V^{+} cells among CFSE^{+} T cells in the spleen of WT or *Sirpa*$^{\Delta DC}$ recipient mice as in F at 1 h after cell transfer. Data are mean ± SE values for three to five mice per group in two to four independent experiments (*A–C* and *E–G*), or for 413 (WT→WT) or 238 (*Cd47* $^{-/-}$→WT) cells from three mice per group (*D*). *P < 0.05, **P < 0.01, ***P < 0.001 by Student's t test (*B–E*), one-way ANOVA and Tukey's test (*F* and *G*), or two-way ANOVA and Sidak's test (*A*).

WT mice. The frequency of transferred *Cd47*$^{-/-}$ T cells was significantly recovered in the spleen of *Sirpa*$^{\Delta DC}$ recipient mice at 24 h after transfusion compared with that apparent for WT recipient mice (Fig. 5*F*). Moreover, the percentage of Annexin V^{+} cells among transferred *Cd47*$^{-/-}$ T cells at 1 h after injection was significantly smaller in *Sirpa*$^{\Delta DC}$ recipient mice compared with WT recipient mice (Fig. 5*G*). Together, these results suggested that SIRPα, a receptor for CD47, in cDCs is also important for the elimination of and induction of cell death in T cells of *Cd47*$^{\Delta T}$ mice.

Direct Interaction of DCs with CD47-Deficient T Cells Induces DC Activation and T Cell Death. We next investigated whether DCs indeed promote necroptosis of CD47-deficient T cells through direct interaction. To this end, we set up an in vitro culture for T cells isolated from the spleen and pLNs of WT or *Cd47*$^{-/-}$ mice together with BM–derived DCs (BMDCs) from WT mice (Fig. 6*A*). Culture of WT T cells with or without BMDCs for 24 h did not result in a significant change in the number of viable T cells (Fig. 6*B*). Culture of *Cd47*$^{-/-}$ T cells alone also did not affect their number, whereas coculture of *Cd47*$^{-/-}$ T cells with BMDCs resulted in a marked reduction in the number of viable T cells (Fig. 6*B*). In addition, the frequency of Annexin V^{+} cells was significantly increased after culture of *Cd47*$^{-/-}$ T cells with BMDCs for 3 h, compared with that apparent after similar coculture of WT T cells (Fig. 6*C*). The expression of CD86 in BMDCs was also increased by coculture with *Cd47*$^{-/-}$ T cells relative to that with WT T cells (Fig. 6*D*). To examine whether the loss of *Cd47*$^{-/-}$ T cells induced by coculture with BMDCs was indeed attributable to necroptosis, we tested the effect of Nec-1. Indeed, Nec-1 significantly attenuated the loss of viable *Cd47*$^{-/-}$ T cells cocultured with BMDCs, whereas treatment with either the pancaspase inhibitor z-VAD-FMK or ferrostatin (Fer-1), an

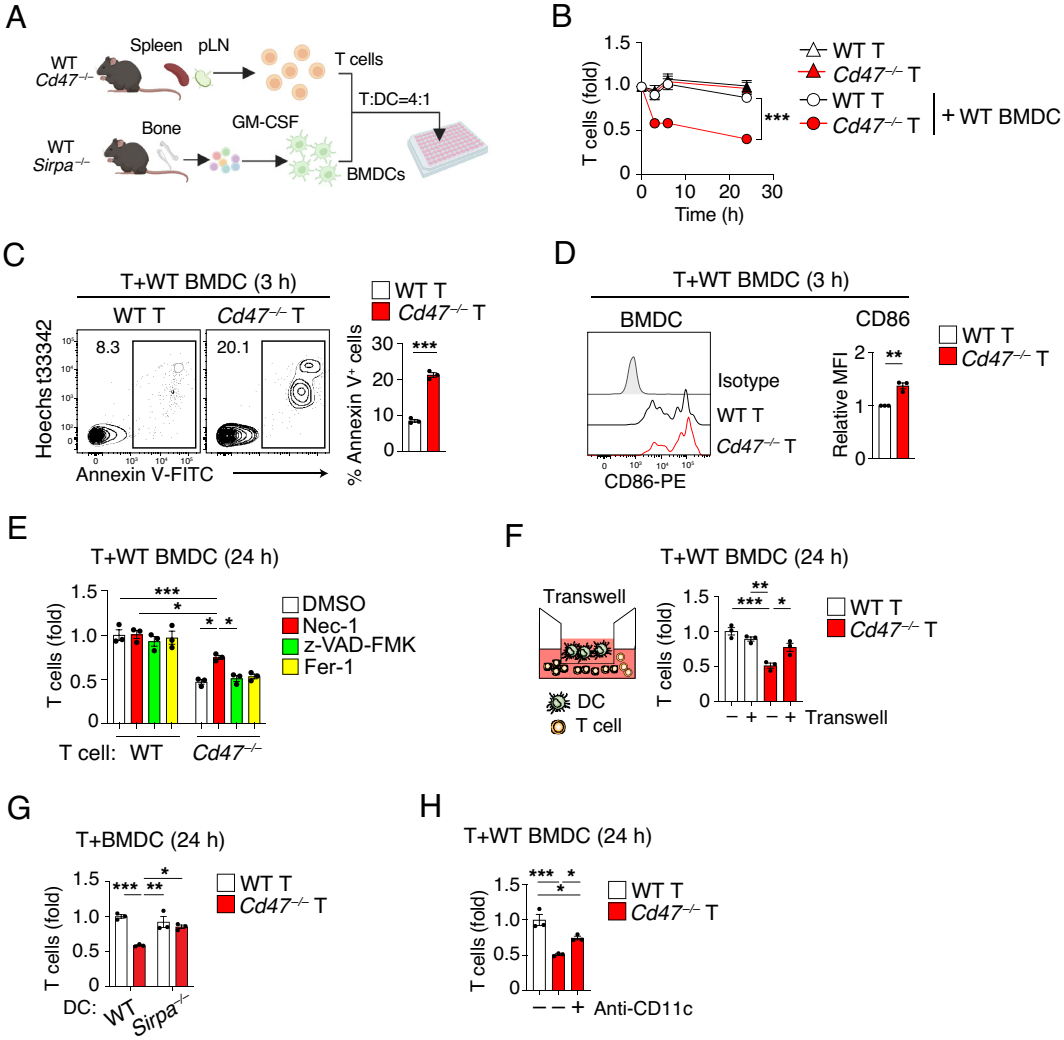

Fig. 6. Direct interaction of DCs with CD47-deficient T cells induces DC activation and T cell death. (*A*) Experimental procedure for T cell–DC coculture. (*B*) WT or *Cd47*$^{-/-}$ T cells were cultured with or without WT BMDCs for the indicated times, after which the number of viable T cells was determined by flow cytometry and normalized relative to the value for time 0. (*C*) The frequency of Annexin V^{+} T cells was determined at 3 h for cocultures as in (*B*). (*D*) Representative plot (*Left*) as well as relative MFI (*Right*) for CD86 expression in BMDCs determined at 3 h for cocultures as in (*B*). (*E*) T cells isolated from WT or *Cd47*$^{-/-}$ mice were cultured for 24 h with BMDCs from WT mice in the presence of DMSO, Nec-1, z-VAD-FMK, or Fer-1, after which the number of viable T cells was determined by flow cytometry and normalized relative to the number for WT T cells in cocultures with DMSO. (*F*) T cells from WT or *Cd47*$^{-/-}$ mice were cultured with WT BMDCs either directly together (−) or separated by a Transwell filter (+) for 24 h, after which the number of viable T cells in the lower chamber was determined and normalized relative to that for WT T cells in conventional cocultures. (*G*) Splenic T cells from WT or *Cd47*$^{-/-}$ mice were cultured for 24 h with BMDCs from WT or *Sirpa*$^{-/-}$ mice, after which the number of viable T cells was determined and normalized relative to that for WT T cell–BMDC cocultures. (*H*) T cells isolated from WT or *Cd47*$^{-/-}$ mice were cultured for 24 h with WT BMDCs in the absence (–, isotype control) or presence of anti-CD11c antibody, after which the number of viable T cells was determined and normalized relative to that for cocultures with WT T cells and without the antibody. Data are mean ± SE values for six-to-nine samples per group in three independent experiments (*B*), or for triplicate determinations from one of three separate experiments (*C*–*H*). **P* < 0.05, ***P* < 0.01, ****P* < 0.001 by two-way ANOVA and Sidak's test (*B*), Student's *t* test (*C* and *D*), or one-way ANOVA and Tukey's test (*E*–*H*).

inhibitor of ferroptosis, failed to do so (Fig. 6*E*). These results suggested that ablation of CD47 in T cells alone is not sufficient to induce cell death, with DCs being required to promote necroptotic cell death of CD47-deficient T cells. To examine whether direct interaction of DCs with CD47-deficient T cells is required for induction of cell death in the latter cells, we cultured the two types of cells in the separate chambers of a Transwell plate. Indeed, separate culture of *Cd47*$^{-/-}$ T cells in the lower chamber with BMDCs in the upper chamber markedly attenuated the loss of viable *Cd47*$^{-/-}$ T cells apparent in conventional cocultures (Fig. 6*F*). The promotion of CD47-deficient T cell death by DCs thus likely requires their direct interaction.

We then examined whether SIRPα in DCs is also important for the depletion of *Cd47*$^{-/-}$ T cells during coculture with BMDCs. Coculture with BMDCs derived from *Sirpa*$^{-/-}$ mice did not induce the loss of *Cd47*$^{-/-}$ T cells apparent during coculture with WT BMDCs (Fig. 6 *A* and *G*). CD11c (also known as integrin α_X) is thought to be important for the activation of cDCs, which is likely induced by the transfer of CD47-deficient RBCs to WT recipient mice (18). We therefore examined whether CD11c also contributes to the loss of *Cd47*$^{-/-}$ T cells induced by culture with WT BMDCs. Indeed, a neutralizing antibody to CD11c significantly attenuated the reduction in the number of *Cd47*$^{-/-}$ T cells in such cocultures (Fig. 6*H*), suggesting that CD11c is required for the depletion of *Cd47*$^{-/-}$ T cells induced by their coculture with BMDCs.

Attenuated Development of Contact Hypersensitivity and Increased Syngeneic Tumor Growth in *Cd47*$^{\Delta T}$ Mice. To explore the importance of CD47 for the promotion of T cell survival under inflammatory conditions, we examined the susceptibility of *Cd47*$^{\Delta T}$ mice to contact hypersensitivity (CHS) induced by 2,4-dinitro-1-fluorobenzene (DNFB) (Fig. 7*A*). Ear thickness after challenge with DNFB was markedly reduced in *Cd47*$^{\Delta T}$ mice compared with *Cd47*$^{f/f}$ mice (Fig. 7*B*). The number of CD4$^+$ T cells in the challenged ear or in cervical LNs (cLNs) was much smaller for *Cd47*$^{\Delta T}$ mice than for *Cd47*$^{f/f}$ mice (Fig. 7*C* and S6*A*). In addition, the number of interferon (IFN)–γ$^+$ or interleukin–17A$^+$ CD4$^+$ T cells [T helper 1 and 17 (Th1 and Th17) cells, respectively] in the challenged ear was markedly decreased in *Cd47*$^{\Delta T}$ mice compared with *Cd47*$^{f/f}$ mice (*SI Appendix*, Fig. S6*B*). The frequency of Annexin V$^+$ cells among as well as the abundance of phosphorylated MLKL in CD4$^+$ T cells of cLNs was significantly increased for *Cd47*$^{\Delta T}$ mice (*SI Appendix*, Fig. S6 *C* and *D*). Treatment with Nec-1 during sensitization significantly enhanced the CHS response in *Cd47*$^{\Delta T}$ mice (Fig. 7*D*). Consistent with this finding, Nec-1 treatment significantly reduced the frequency of Annexin V$^+$ CD4$^+$ T cells in cLNs of *Cd47*$^{\Delta T}$ mice (Fig. 7*E*). Moreover, the number of CD4$^+$ T cells was markedly increased in the DNFB-challenged ear by Nec-1 treatment in *Cd47*$^{\Delta T}$ mice (*SI Appendix*, Fig. S6*E*). These results suggested that ablation of CD47 specifically in T cells resulted in a marked defect in the generation of CD4$^+$ Th1 or Th17 cells and the consequent CHS response.

We also examined the activity of cytotoxic T cells (CTLs) in *Cd47*$^{\Delta T}$ mice with the use of the MC38 colorectal tumor model, for which CTLs are implicated in antitumor immunity (33). We observed that MC38 tumor growth was markedly increased in *Cd47*$^{\Delta T}$ mice compared with *Cd47*$^{f/f}$ mice (Fig. 7*F*). Indeed, the frequency of CD8$^+$ T cells infiltrated into the tumors as well as in tumor-draining LNs (tdLNs) was greatly reduced in *Cd47*$^{\Delta T}$ mice (Fig. 7*G* and *SI Appendix*, Fig. S6*F*). In addition, the frequency of tumor-infiltrating CD8$^+$ T cells positive for IFN-γ was significantly decreased (Fig. 7*H*), whereas the expression of PD-1 on these cells was increased (*SI Appendix*, Fig. S6*G*), in *Cd47*$^{\Delta T}$ mice compared with *Cd47*$^{f/f}$ mice. Furthermore, the frequency of Annexin V$^+$ cells among (Fig. 7*I*) as well as the abundance of phosphorylated MLKL in (*SI Appendix*, Fig. S6*H*) CD8$^+$ T cells of tdLNs was significantly increased in *Cd47*$^{\Delta T}$ mice compared with *Cd47*$^{f/f}$ mice. Collectively, these results suggested that ablation of CD47 in T cells also resulted in a marked defect in the generation of CD8$^+$ CTLs as well as attenuated their inhibitory effect on MC38 tumor formation.

Discussion

With the use of T cell–specific CD47-deficient (*Cd47*$^{\Delta T}$) mice, we have here shown that specific depletion of CD47 in T cells resulted in the cDC-mediated cell death of peripheral T cells and impairment of their adaptive immune responses. Such regulation by cDCs likely contributes to the survival and homeostasis of peripheral T cells (34). Moreover, we found that the remaining peripheral T cells in *Cd47*$^{\Delta T}$ mice were activated and that the frequency of their cell death and their turnover were both increased. Morphological and biochemical characterization of these remaining T cells in *Cd47*$^{\Delta T}$ mice revealed that their cell death was likely attributable to necroptosis, a caspase-independent type of cell death that occurs in pathogenic or inflammatory conditions (35, 36). Indeed, RNA-seq analysis of sorted T cells from the spleen of *Cd47*$^{\Delta T}$ mice showed enrichment for gene sets related to the inflammatory response or cell death. Induction of necroptosis requires death receptors such as Fas or members of the tumor necrosis factor receptor (TNFR) family (37). These changes in the remaining T cells are thought to be caused by necroptosis of T cells, and we indeed demonstrated recovery of peripheral T pool after the Nec-1 treatment in *Cd47*$^{\Delta T}$ mice. However, we cannot exclude the possibility that some phenotypical changes of T cells in *Cd47*$^{\Delta T}$ mice were, at least in part, attributable to the different CD4 and CD8 ratios, as well as skewed phenotype from naïve to memory phenotype, of remaining T cells. In addition, the development of thymocytes was intact in *Cd47*$^{\Delta T}$ mice, even though the expression of CD47 was diminished during the development of T cells in the thymus. Moreover, the transient transfer of *Cd47*$^{-/-}$ T cells into WT mice resulted in their cell death and rapid elimination. Together, our results suggest that the marked reduction in the number of T cells in peripheral tissues of *Cd47*$^{\Delta T}$ mice occurs after the egress of T cells from the thymus, and is thus not attributable to an impairment of T cell development in the thymus as a result of constitutive CD47 deficiency.

The marked depletion of T cells caused by necroptotic cell death in *Cd47*$^{\Delta T}$ mice appeared to require cDCs, in particular cDC2s. Indeed, this cell death as well as the loss of T cells apparent in *Cd47*$^{\Delta T}$ mice were partially attenuated by the depletion of cDCs in *Cd47*$^{\Delta T}$;CD11c$^{iDTR\Delta}$ mice. Moreover, cDC2s, but not cDC1s, were markedly activated and decreased in number as well as showed increased expression of FasL in SLOs of *Cd47*$^{\Delta T}$ mice. Transient transfer of *Cd47*$^{-/-}$ RBCs was previously shown to result in the activation and loss of cDC2s in SLOs of WT recipient mice (17, 18). The rapid clearance of *Cd47*$^{-/-}$ T cells transferred to WT recipient mice observed in the present study was also attenuated by the depletion of cDCs in CD11c$^{iDTR\Delta}$ mice. Taken together, these findings suggest that the interaction of CD47-deficient T cells with cDC2s resulted in activation of the latter cells, which in turn promoted the necroptotic cell death of the former cells, in *Cd47*$^{\Delta T}$ mice. Of note, cDC2s remained active after the NEC-1 treatment in *Cd47*$^{\Delta T}$ mice, in which T cells escaped from necroptotic cell death by the treatment, suggesting that such activation

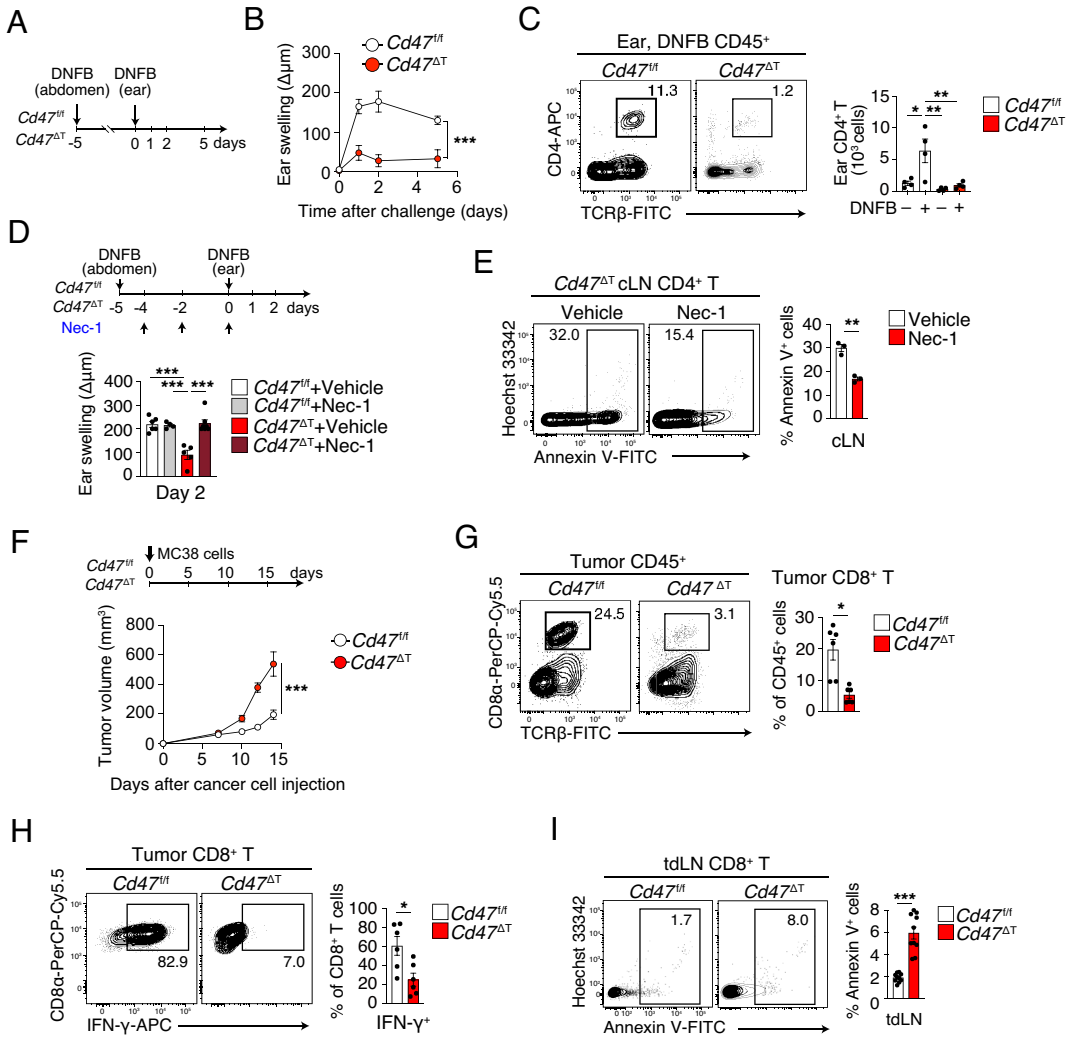

Fig. 7. Attenuated development of CHS and increased syngeneic tumor growth in *Cd47*$^{\Delta T}$ mice. (*A*) Experimental scheme for a DNFB-induced CHS model. (*B*) Ear thickness was measured at 0, 1, 2, and 5 d after DNFB challenge in sensitized mice. An increase in ear thickness (swelling) was defined as the difference in thickness between DNFB-treated and vehicle-treated ears. (*C*) Representative flow cytometry plots (*Left*) and the absolute number (*Right*) of CD4$^+$ T cells among ear-infiltrating CD45$^+$ cells at 2 d after DNFB challenge in *Cd47*$^{f/f}$ or *Cd47*$^{\Delta T}$ mice. Sensitized mice were challenged with vehicle (–DNFB) as a control. (*D*) Ear thickness measured at 2 d after DNFB challenge in sensitized *Cd47*$^{f/f}$ or *Cd47*$^{\Delta T}$ mice that had been injected intravenously with Nec-1 or vehicle every other day beginning at day –4. (*E*) Representative plots (*Left*) and the percentage (*Right*) of Annexin V$^+$ cells among CD4$^+$ T cells in cLNs at 2 d after DNFB challenge in sensitized *Cd47*$^{\Delta T}$ mice also treated with Nec-1 or vehicle. (*F*) Time course of tumor volume in *Cd47*$^{f/f}$ or *Cd47*$^{\Delta T}$ mice injected subcutaneously with MC38 cells on day 0. (*G*) Representative flow cytometry plots (*Left*) and the percentage (*Right*) of CD8$^+$ T cells among CD45$^+$ cells isolated from MC38 tumors at 14 d after cell injection. (*H*) Representative plots (*Left*) and the percentage (*Right*) of IFN-γ$^+$ cells among tumor-infiltrating CD8$^+$ T cells isolated at 14 d after MC38 cell injection and ex vivo restimulation. (*I*) Representative plots (*Left*) and the percentage (*Right*) of Annexin V$^+$ cells among CD8$^+$ T cells in tdLNs at 14 d after MC38 cell injection. Data are mean ± SE values for three-to-four mice per group from three independent experiments (*B*–*E*), or for six-to-ten mice per group in two or three independent experiments (*F*–*I*). *P < 0.05, **P < 0.01, ***P < 0.001 by two-way ANOVA and Sidak's test (*B* and *F*), Student's *t* test (*E* and *G*–*I*), or one-way ANOVA and Tukey's test (*C* and *D*).

of cDC2s is not induced as a consequence of T cell death in *Cd47*$^{\Delta T}$ mice. With the use of in vitro coculture of T cells and BMDCs, we indeed showed that the direct interaction of *Cd47*$^{-/-}$ T cells with WT BMDCs resulted in induction of necroptotic death of the former cells as well as in activation of the latter cells.

The mechanism by which CD47-deficient T cells first trigger the activation of cDC2s remains unclear. The binding of CD47 on T cells to SIRPα on cDCs is thought to result in the tyrosine phosphorylation of the cytoplasmic immunoreceptor tyrosine-based inhibition motif region of SIRPα and recruitment of the protein tyrosine phosphatase Shp1, which prevents the excessive activation of DCs (38, 39). Deficiency of CD47 in T cells may therefore trigger the activation of interacting cDCs. Consistent with this notion, SIRPα is preferentially expressed on cDC2s among cDC subtypes (22), and the activation of cDCs in *Cd47*$^{\Delta T}$ mice was also restricted to cDC2s. By contrast, CD47 on RBCs has been thought to inhibit the activity of an as yet unidentified ligand required for activation of macrophages or cDCs (40). We indeed found that an antibody to CD11c (integrin α_X) attenuated the loss of *Cd47*$^{-/-}$ T cells induced by coculture with WT BMDCs. Similar to the situation with CD47-deficient RBCs (18), it is thus likely that a ligand for CD11c, the expression or function of which is inhibited by CD47, participates in the activation of cDCs by CD47-deficient T cells. In addition, it remains unclear whether cDC2s induce cell death of CD47–deficient cells other than peripheral T cells and RBCs, particularly in the steady state. Further study is necessary to understand the role of CD47–SIRPα signaling in the regulation of blood/immune cell survival.

Of note, the marked reduction in the number and increase in the extent of cell death of *Cd47*$^{-/-}$ T cells apparent on their transfer to WT recipient mice was not observed on their transfer to *Sirpa*$^{\Delta DC}$ mice. Not only cDCs per se but also the expression of SIRPα in these cells are therefore important for the marked reduction in the number

of peripheral T cells caused by their cell death in *Cd47*$^{\Delta T}$ mice. The mechanism underlying the prevention of T cell deficiency in *Cd47*$^{\Delta T}$ mice by depletion of SIRPα in cDCs remains unknown. However, the number of cDC2s, but not that of cDC1s, was previously shown to be greatly decreased in SLOs of cDC-specific SIRPα-deficient (*Sirpa*$^{\Delta DC}$) mice (6, 32). Moreover, the ability of cDC2s from *Sirpa*$^{\Delta DC}$ mice to produce TNFR ligands such as TNF-α (41), which is thought to be important for the induction of necroptosis in target cells (37), was found to be markedly reduced (6). Taken together, these observations suggest that cDC2s are indeed effector cells for the induction of necroptotic cell death in CD47-deficient T cells in a manner dependent on their direct interaction.

We also showed that the expression of CD47 on T cells is indeed important for their immunological function including the development of hypersensitivity mediated by CD4$^+$ Th cells and the inhibition of tumor growth mediated by cytotoxic CD8$^+$ T cells. Downregulation of CD47 expression was previously described in aged RBCs (42, 43) and HIV-infected CD4$^+$ T cells (44). It is likely that the reduction in the number of HIV-infected T cells is in part attributable to their cDC-mediated necroptotic cell death. In contrast, the expression of CD47 is thought to increase markedly in a variety of cancer types including T cell leukemia (45, 46). Given that CD47 expression in such cancer cells may also prevent their DC-mediated cell death, the high expression of CD47 in cancer cells likely promotes their survival and proliferation. Depletion of CD47 by genetic manipulation with the use of small interfering RNAs or microRNAs may therefore be a promising strategy for the treatment of cancers that express CD47 at a high level.

Materials and Methods

Animals, antibodies and reagents, cell preparation and flow cytometry, mixed BM chimeras, determination of BrdU incorporation, analysis of cell cycle profile and cell death, RNA-seq analysis, RT-qPCR analysis, May–Grünwald–Giemsa staining, TEM, depletion of DCs, granulocytes, NK cells, and macrophages, immunohistofluorescence analysis, adoptive transfer of T cells, generation of GM-CSF-induced BMDCs, coculture of BMDCs with T cells, induction of CHS, MC38 cell engraftment, and statistical analysis can be found in *SI Appendix, Materials and Methods*. All animal experiments were approved by the animal care and experimentation committees of Kobe University (permit no. P201003).

Data, Materials, and Software Availability. All study data are included in the article and/or *SI Appendix*. Data generated in this study are available in the Genomic Expression Archive (GEA) database for bulk RNA-seq data under accession no. GSE224426 (47).

ACKNOWLEDGMENTS. We thank N. Hasegawa, Y. Takase, Y. Kanno, Y. Matozaki, and D. Tanaka for technical assistance; H. Kayama and K. Takeda (Osaka University) for providing CD11c^{iDTR} mice; M. Nishio and A. Suzuki (Kobe University) for technical support in animal experiments; as well as K. Matsushita, M. Taniguchi, and T. Furuyashiki (Kobe University) for technical advice for RNA-seq analysis. This work was supported by a Grant-in-Aid for Scientific Research (A) (21H04807 to T.M.), a Grant-in-Aid for Scientific Research (C) (22K08504 to Y.S.), and a Grant-in-Aid for Young Scientist (22K15494 to S.K.) from Japan Society for the Promotion of Science (JSPS); by P-CREATE (21cm0106308h0006) and P-PROMOTE (22674074) grants (to T.M. and Y.S.) of the Japan Agency for Medical Research and Development; by COI-NEXT grant (JPMJPF2018) of Japan Science and Technology Agency; and in part by grants from the Yasuda Medical Foundation and Chugai Foundation for Innovative Drug Discovery Science (to T.M.) and from Senshin Medical Research Foundation (to Y.S.) and by a donation from Dr. T. Yamao (to Kobe University). S.K. was also supported by JSPS Research Fellowships for Young Scientists and a scholarship from Nakatani Foundation for Advancement of Measuring Technologies in Biomedical Engineering.

Author affiliations: [a]Division of Biosignal Regulation, Department of Biochemistry and Molecular Biology, Kobe University Graduate School of Medicine, Kobe 650-0047, Japan; [b]Division of Molecular and Cellular Signaling, Department of Biochemistry and Molecular Biology, Kobe University Graduate School of Medicine, Kobe 650-0017, Japan; [c]Division of Reconstruction, Oculoplasty, and Oncology, Department of Ophthalmology, Faculty of Medicine, Public Health, and Nursing, Gadjah Mada University, Yogyakarta 55281, Indonesia; [d]Division of Structural Medicine and Anatomy, Department of Physiology and Cell Biology, Kobe University Graduate School of Medicine, Kobe 650-0017, Japan; [e]Department of Nephrology and Rheumatology, Gunma University Graduate School of Medicine, Gunma 371-8511, Japan; and [f]Department of Laboratory Sciences, Gunma University Graduate School of Health Sciences, Gunma 371-8514, Japan

1. R. M. Steinman, Decisions about dendritic cells: Past, present, and future. *Annu. Rev. Immunol.* **30**, 1–22 (2012).
2. M. Cabeza-Cabrerizo, A. Cardoso, C. M. Minutti, M. P. da Costa, C. R. e Sousa, Dendritic cells revisited. *Annu. Rev. Immunol.* **39**, 131–166 (2021).
3. A. Roquilly, J. D. Mintern, J. A. Villadangos, Spatiotemporal adaptations of macrophage and dendritic cell development and function. *Annu. Rev. Immunol.* **40**, 525–557 (2022).
4. H. Hasegawa, T. Matsumoto, Mechanisms of tolerance induction by dendritic cells In vivo. *Front. Immunol.* **9**, 350 (2018).
5. L. Klein, B. Kyewski, P. M. Allen, K. A. Hogquist, Positive and negative selection of the T cell repertoire: What thymocytes see (and don't see). *Nat. Rev. Immunol.* **14**, 377–391 (2014).
6. Y. Saito *et al.*, SIRPα+ dendritic cells regulate homeostasis of fibroblastic reticular cells via TNF receptor ligands in the adult spleen. *Proc. Natl. Acad. Sci. U.S.A.* **114**, E10151–E10160 (2017).
7. V. Kumar *et al.*, A dendritic-cell-stromal axis maintains immune responses in lymph nodes. *Immunity* **42**, 719–730 (2015).
8. E. J. Brown, W. A. Frazier, Integrin-associated protein (CD47) and its ligands. *Trends Cell Biol.* **11**, 130–135 (2001).
9. T. Matozaki, Y. Murata, H. Okazawa, H. Ohnishi, Functions and molecular mechanisms of the CD47–SIRPα signalling pathway. *Trends Cell Biol.* **19**, 72–80 (2009).
10. A. N. Barclay, T. K. van den Berg, The interaction between signal regulatory protein alpha (SIRPα) and CD47: Structure, function, and therapeutic target. *Annu. Rev. Immunol.* **32**, 25–50 (2014).
11. M. E. W. Logtenberg, F. A. Scheeren, T. N. Schumacher, The CD47-SIRPα immune checkpoint. *Immunity* **52**, 742–752 (2020).
12. P.-A. Oldenborg *et al.*, Role of CD47 as a marker of self on red blood cells. *Science* **288**, 2051–2054 (2000).
13. Z. Bian *et al.*, Cd47-Sirpα interaction and IL-10 constrain inflammation-induced macrophage phagocytosis of healthy self-cells. *Proc. Natl. Acad. Sci. U.S.A.* **113**, E5434–E5443 (2016).
14. T. Ishikawa-Sekigami *et al.*, SHPS-1 promotes the survival of circulating erythrocytes through inhibition of phagocytosis by splenic macrophages. *Blood* **107**, 341–348 (2006).
15. T. Ishikawa-Sekigami *et al.*, Enhanced phagocytosis of CD47-deficient red blood cells by splenic macrophages requires SHPS-1. *Biochem. Biophys. Res. Commun.* **343**, 1197–1200 (2006).
16. P.-A. Oldenborg, H. D. Gresham, F. P. Lindberg, Cd47-signal regulatory protein α (Sirpα) regulates Fcγ and complement receptor–mediated phagocytosis. *J. Exp. Med.* **193**, 855–862 (2001).
17. T. Yi *et al.*, Splenic dendritic cells survey red blood cells for missing self-CD47 to trigger adaptive immune responses. *Immunity* **43**, 764–775 (2015).
18. J. Wu, H. Wu, J. An, C. M. Ballantyne, J. G. Cyster, Critical role of integrin CD11c in splenic dendritic cell capture of missing-self CD47 cells to induce adaptive immunity. *Proc. Natl. Acad. Sci. U.S.A.* **115**, 6786–6791 (2018).
19. H. Wang *et al.*, Lack of CD47 on nonhematopoietic cells induces split macrophage tolerance to CD47null cells. *Proc. Natl. Acad. Sci. U.S.A.* **104**, 13744–13749 (2007).
20. B. R. Blazar *et al.*, CD47 (integrin-associated protein) engagement of dendritic cell and macrophage counterreceptors is required to prevent the clearance of donor lymphohematopoietic cells. *J. Exp. Med.* **194**, 541–550 (2001).
21. X. Wang *et al.*, TCR-dependent transformation of mature memory phenotype T cells in mice. *J. Clin. Invest.* **121**, 3834–3845 (2011).
22. Y. Saito *et al.*, Regulation by SIRPα of dendritic cell homeostasis in lymphoid tissues. *Blood* **116**, 3517–3525 (2010).
23. D. Tang, R. Kang, T. V. Berghe, P. Vandenabeele, G. Kroemer, The molecular machinery of regulated cell death. *Cell Res.* **29**, 347–364 (2019).
24. S. Bedoui, M. J. Herold, A. Strasser, Emerging connectivity of programmed cell death pathways and its physiological implications. *Nat. Rev. Mol. Cell Biol.* **21**, 678–695 (2020).
25. D. Ofengeim, J. Yuan, Regulation of RIP1 kinase signalling at the crossroads of inflammation and cell death. *Nat. Rev. Mol. Cell Biol.* **14**, 727–736 (2013).
26. A. Kaczmarek, P. Vandenabeele, D. V. Krysko, Necroptosis: The release of damage-associated molecular patterns and its physiological relevance. *Immunity* **38**, 209–223 (2013).
27. L. Sun *et al.*, Mixed lineage kinase domain-like protein mediates necrosis signaling downstream of RIP3 kinase. *Cell* **148**, 213–227 (2012).
28. N. Garbi, T. Kreutzberg, Dendritic cells enhance the antigen sensitivity of T cells. *Front. Immunol.* **3**, 389 (2012).
29. M. Okuyama *et al.*, A novel in vivo inducible dendritic cell ablation model in mice. *Biochem. Biophys. Res. Commun.* **397**, 559–563 (2010).
30. R. A. Wilcox *et al.*, Cutting edge: Expression of functional CD137 receptor by dendritic cells. *J. Immunol.* **168**, 4262–4267 (2002).
31. T. Yi, J. G. Cyster, EBI2-mediated bridging channel positioning supports splenic dendritic cell homeostasis and particulate antigen capture. *ELife* **2**, e00757 (2013).
32. K. Washio *et al.*, Dendritic cell SIRPα regulates homeostasis of dendritic cells in lymphoid organs. *Genes Cells* **20**, 451–463 (2015).
33. X. Liu *et al.*, CD47 blockade triggers T cell–mediated destruction of immunogenic tumors. *Nat. Med.* **21**, 1209–1215 (2015).

34. C. D. Surh, J. Sprent, Homeostasis of naive and memory T cells. *Immunity* **29**, 848–862 (2008).
35. M. E. Choi, D. R. Price, S. W. Ryter, A. M. K. Choi, Necroptosis: A crucial pathogenic mediator of human disease. *JCI Insight* **4**, e128834 (2019).
36. I. L. Ch'en, J. S. Tsau, J. D. Molkentin, M. Komatsu, S. M. Hedrick, Mechanisms of necroptosis in T cells. *J. Exp. Med.* **208**, 633–641 (2011).
37. A. G. Snyder, A. Oberst, The antisocial network: Cross talk between cell death programs in host defense. *Annu. Rev. Immunol.* **39**, 77–101 (2021).
38. T. Kaneko *et al.*, Dendritic cell-specific ablation of the protein tyrosine phosphatase Shp1 promotes Th1 cell differentiation and induces autoimmunity. *J. Immunol.* **188**, 5397–5407 (2012).
39. C. L. Abram, G. L. Roberge, L. I. Pao, B. G. Neel, C. A. Lowell, Distinct roles for neutrophils and dendritic cells in inflammation and autoimmunity in motheaten mice. *Immunity* **38**, 489–501 (2013).
40. D. Liu, L. Duan, J. G. Cyster, Chemo- and mechanosensing by dendritic cells facilitate antigen surveillance in the spleen. *Immunol. Rev.* **306**, 25–42 (2022).
41. C. C. Brown *et al.*, Transcriptional basis of mouse and human dendritic cell heterogeneity. *Cell* **179**, 846–863.e24 (2019).
42. S. Khandelwal, N. V. Rooijen, R. K. Saxena, Reduced expression of CD47 during murine red blood cell (RBC) senescence and its role in RBC clearance from the circulation. *Transfusion* **47**, 1725–1732 (2007).
43. F. Wang *et al.*, Aging-associated changes in CD47 arrangement and interaction with thrombospondin-1 on red blood cells visualized by super-resolution imaging. *Aging Cell* **19**, e13224 (2020).
44. L. Cong *et al.*, HIV-1 Vpu promotes phagocytosis of Infected CD4+ T cells by macrophages through downregulation of CD47. *Mbio* **12**, e0192021 (2021).
45. K. Müller *et al.*, Combining daratumumab with CD47 blockade prolongs survival in preclinical models of pediatric T-ALL. *Blood* **140**, 45–57 (2022).
46. Y. Murata, Y. Saito, T. Kotani, T. Matozaki, CD47-signal regulatory protein α signaling system and its application to cancer immunotherapy. *Cancer Sci.* **109**, 2349–2357 (2018).
47. Y. Saito, CD47 promotes peripheral T cell survival by preventing dendritic cell–mediated T cell necroptosis. NBCI GEO. https://www.ncbi.nlm.nih.gov/geo/query/acc.cgi?acc=GSE224426. Deposited 3 February 2023.